Region Wise Surface Level Defect Detection and Ranking of Crust Leather Images Based on Image Processing Techniques

by

S. Nithiyanantha Vasagam[a,b] and M. Sornam[a*]

[a]*Department of Computer Science, University of Madras, Guindy Campus,* Chennai – 600025, Tamil Nadu, India

[b]*Knowledge Portfolio Management Department, Council of Scientific & Industrial Research (CSIR) - Central Leather Research Institute (CLRI),* Adyar, Chennai – 600020, Tamil Nadu, India

Abstract

Sorting and aligning of crust leather for grading on position wise defect distribution is one of the methods adopted in the tanning industry. This method is generally carried out manually by a veteran on official sampling position and their input is critical because it is directly linked to sales of the crust leather. The opinion of the experts is believed to be stable and consumes a good amount of time too. Hence, in the current research a robust defect detection method and ranking of crust leather images based on image processing techniques is proposed to give a stable solution in a short span of time. A custom-made dataset of crust leather images consisting of 5640 images were used in this study. The pixel intensity has been extracted on demarcated position of various regions including neck, belly left, belly right, center and butt instead of official sampling position through horizontal and vertical mapping of coordinates with a new method Grading Score on Image Position wise (GSIP) on the actual images. The image processing techniques using Canny Edge Detection and filters such as Laplacian, Median, Prewitt, Roberts, Sobel and Scharr were implemented to get the pixel intensity grouped and classified based on parameters within acceptable range using a Naïve Bayes Classifier. The classifier confirms that the accuracy of Set I - Actual Images and Set II - Defects with implementation of canny edge detection over other image processing techniques at 99.50%. Therefore, the current research confirms that the proposed GSIP method would give an additional tool to inspectors while ranking the crust leather based on region wise surface level defect detection of crust leather images based on image processing techniques.

Introduction

Leather is a by-product of the meat industry and annually the international trade is estimated to be about US$ 80 billion.[1] The conventional process associated in making leather starts from the initial stage of collection of raw hides & skins, then soaking, liming, fiber opening (re-liming), fleshing, deliming, pickling, chrome tanning, splitting & shaving, post tanning (crust leather)[2] and ends up with the stage called finishing.[3] Finished leather is further processed for the making of leather footwear, leather garments, leather goods and saddlery & harness. The value of the finished leather is determined depending upon the observations[4] made on the surface on official sampling positions of the crust leather. The role of inspectors is to observe the surface level[5] and it is the key which basically determines the value of the finished leather. Experts usually segregate upon the ranking like 1, 2, 3, 4, 5, 6, 7 and R. Normally, the rank 1-2 will go into high-end products, 3-4 will go into mid-range products and 5-6 will go for low range products and the R will be considered for direct rejection.[6,7]

To extract some useful information, the image processing technique is applied on an image with Edge Detection and Filters. Yang Liu et al.[8] has presented an adaptive, robust and effective edge detector and described edge points as strong edge, pixels, weak edge pixels and non-edge pixels depend on the gradients while segmentation with Canny algorithm. Gandhi et al.[9] applied Canny edge detection on images of letters placed on ground and captured through drone cameras. The Canny edge detector[10] goes a step further by employing non-maximum suppression to extract a thinner contour and applying the double threshold algorithm to get the weak edges. However, it is difficult to get a suitable threshold, especially in a dynamic environment where the background changes rapidly. To extract the structural details Canny edge detection[11] technique is applied based on double threshold algorithm to extract a thinner contour even on the weak edges in all real edges which is shown in Equation 1.

$$\blacktriangledown (Ga * Im) \text{ where Ga: Gaussian and Im: Image} \quad (1)$$

Filters such as Laplacian, Median, Sobel, Roberts, Scharr and Prewitt detect pixels with brightness, colors and gradients to reduce noise.[12] Laplacian enhances the edges of an image with pixel intensity values. Median filter reduces noise in an image based on pixel intensities. The Sobel calculates the gradient of image intensity on regions of high spatial level of each pixel. Roberts detect the edge of the image. Scharr detects edges deriving by pixel intensity corresponding to gradient edges. Prewitt detects edges based on the pixel intensities of an image in horizontal and vertical directions.

Aslam, M., et al.[13] have reported on inspection methods based on leather surface defects based on deep learning methods. They have mentioned that the market value will be reduced based on significant defects present in raw hides and leather as per the sub-divisions of a hide such as Head, Shoulder, Bend, Belly, Side, Crop,

*Corresponding author email: madasamy.sornam@gmail.com

Manuscript received February 20, 2022, accepted for publication February 27, 2023.

Back, Croupon, Dosset and Culatta. Lai, K., et al.[14] have presented an automated vision system intending to detect and classify surface defects in steel plate. Authors implemented Sobel filter for detecting edges and adopted fuzzy neural network for the defect classification.

Gong, R., et al.[15] have proposed a classifier support vector hyper-spheres with insensitivity to noise (INSVHs) on steel plate surface defects such as hole, scratch, bruise, wave, scarring and scale based on region of defects. Hu, L., et al.[16] have developed a new method to identify steel-plate surface defects such as Common defects consisting of Bumps, Scratches & Oil Spots and non-common defects consisting of Stains & Dirtiness. They have implemented synthetic minority over-sampling technique (SMOTE) and AdaBoost.BK algorithm.

Suvdaa, B., et al.[17] have proposed a framework for exact defect points by forming a single image on the basis of feature vectors in steel surface using Scale Invariant Feature Transform for defects detection and Support Vector Machines for defects classification. Villar, P., et al.[18] have proposed an automatic method for defect classification of the Wet Blue leather from the Gray Scale image, the RGB and HSV color model. The features were extracted based on the Sequential Forward Selection method and classification was implemented using a Supervised Neural Network.

Pistori, H., et al.[19] have suggested defect detection in raw hide and wet blue leather having four different defects such as brand marks, tick marks, cuts and scabies through demerit count reference standard for leather raw hides. They have implemented two tailed, t-student test while classification using support vector machines. Vasagam, S.N., et al.[20] have presented the options of defects Identification of Crust Leathers using Computer-aided Grading by calculating position of defects, extent of defects and the distribution of defects with a Logical table for objective grading.

Liong, S.T., et al.[21] have proposed instance segmentation to distinguish whether the leather sample contains a defective part or not using deep learning to classify the three-categories of leather images. Jian, L., et al.[22] have proposed using Feed-forward Neural Network (FNN) by combining decision trees in defect detection and classify the leather based on surface defects of shape, texture and color. Bong, H.Q., et al.[23] has introduced an automated vision-based system which consists of an image grabbing mechanism on locating position of the leather defects by classifying based on color, shape and texture using the classifier SVM.

Sornam, M. and Vasagam, S.N.[24] had suggested a model to group the Intermittent Leather Images using Linear Discriminant Model as per the category of normal leather and defective leather based on surface level features such as base color, other than base color, share of regions, share of cutting area, share of cutting value, position wise length and position wise breadth. Xie, X., et al.[25] has proposed an improved image matching algorithm of defects by describing spatial signals on navel orange surface based on compressed sensing by combining of wavelet transform (WT) and speeded up robust features (SURF).

Aslam, Y., et al.[26] has proposed an automatic segmentation and quantification approach for inspecting defects on Metal from digital images consisting of input image and ground truth using convolutional neural network (CNN) approach. Vasagam, S.N. and Sornam, M.[27] has proposed an Intermittent Leather Defect Detection based on Outer and Inner radius using Leather Image Surface Feature Extraction LISFE derived from Black Hat transformation

Table I

Summary of Authors, Techniques and Area

S. No	Authors	Name of the Technique/method	Area / Material
1.	Aslam, M., et al.[13]	Deep Learning Methods	Wet blue leather
2.	Lai, K., et al.[14]	Automated Vision System	Steel
3.	Gong, R., et al.[15]	Support Vector Hyper-Spheres with Insensitivity to Noise	Steel
4.	Hu, L., et al.[16]	New method to identify steel-plate surface defect	Steel
5.	Suvdaa, B., et al.[17]	Scale Invariant Feature Transform and Support Vector Machines	Steel
6.	Villar, P., et al.[18]	Sequential Forward Selection method and Supervised Neural Network	Wet Blue leather
7.	Pistori, H., et al.[19]	Sequential Forward Selection and Supervised Neural Network	Raw hide and wet blue leather
8.	Vasagam, S.N., et al.[20]	Computer Aided Grading	Crust Leather
9.	Liong, S.T., et al.[21]	Instance segmentation	Leather
10.	Jian, L., et al.[22]	Feed-forward Neural Network	Leather
11.	Bong, H.Q., et al.[23]	Support Vector Machines	Leather
12.	Sornam, M. and Vasagam, S.N.,[24]	Linear Discriminant Model	Intermittent Leather
13.	Xie, X., et al.[25]	Wavelet Transform and Speeded Up Robust Features	Orange
14.	Aslam, Y., et al.[26]	Convolutional Neural Network	Metal
15.	Vasagam, S.N. and Sornam, M.,[27]	Ensemble Algorithms	Intermittent Leather

and Hough transformation. The majority of the research discussed as shown in Table I in this field had explored classifying the images on the basis of surface level. It shows the importance of studying the images on the surface and indicates that there exists an ample scope in determining the surface level defect detection on region wise on crust leather images based on image processing techniques.

- The authors in the research article have set an objective to give emphasis on region wise surface level defect detection instead of official sampling position and then ranking of the leather images on the basis of position of the region using image processing techniques. The contributions of authors are given below.
- A custom-made dataset of crust leather images consisting of 5640 images consisting of two datasets. Dataset I consists of the original images with truth values, original images applied with Canny Edge Detection and also from Filters such as Laplacian, Median, Prewitt, Roberts, Sobel and Scharr. Dataset II consists of original images with truth values and original images applied with Canny Edge Detection.
- Pixel intensity has been extracted on five regions based on Horizontal and Vertical mapping of coordinates.
- Ranking of crust leather image has been implemented from the extracted feature with the proposed method called Grading Score on Image Position wise (GSIP).
- Classification of ranking by grouping them as "within the acceptable Range" or "Not within the acceptable Range" based on the threshold value set as the individual rank which is less than or equal to threshold value of four with Naïve Bayes classifier.

The manuscript has covered the remaining sections of Methodology, Results & Discussions in the following sections which is represented in Figure 1 and working model is shown in Figure 2.

1. Creation of Dataset I and II
2. Implementation of contour of five regions and applied Canny Edge Detection & Other Filters
3. Feature extracted based on Horizontal and Vertical mapping of coordinates
4. Generation of Ranking Matrix of crust leather image from the extracted feature with the proposed method called Grading Score on Image Position wise (GSIP)
5. Classification of ranking by grouping them as "within the acceptable Range" or "Not within the acceptable Range" based on Naïve Bayes Classifier.

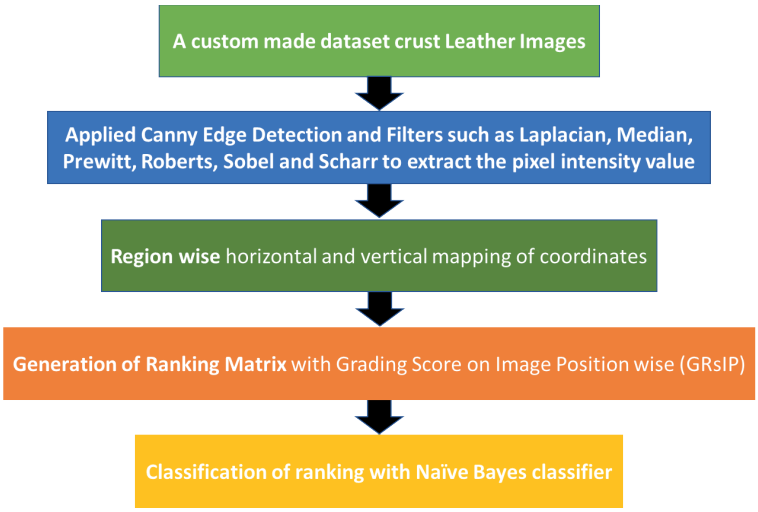

Figure 1. Workflow

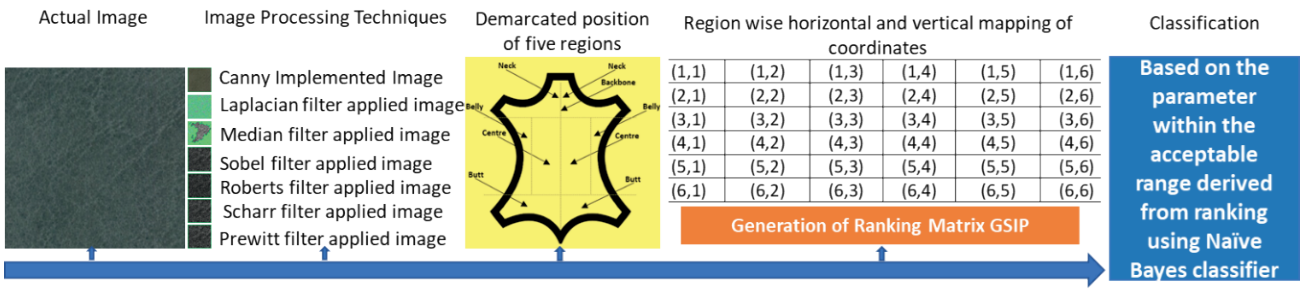

Figure 2. Working Model

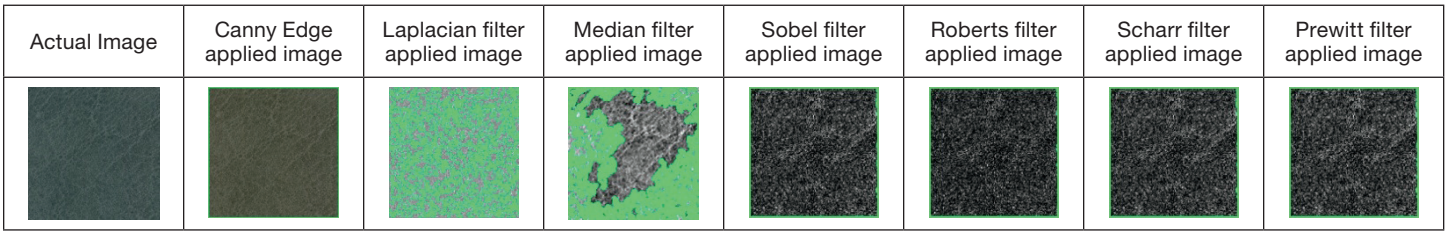

Figure 3. Sample image and filtered images Workflow

Methodology

A. **Dataset of Crust leather images:** Image dataset of Crust leather images in the Set I and Set II consisted of 4872 and 768 respectively. These images were originally taken using a Konica camera and cropped into the size of 250 x 250 with 72 dpi for Set I and 300 x 300 with 96 dpi for Set II. In the Set I image, dataset is consisting of image filtered from actual images from filters such as Laplacian, Median, Sobel, Roberts, Scharr and Prewitt as shown in Figure 3.

B. **Region wise Horizontal and Vertical Mapping - Feature Extraction:** In general, the experts who do the sorting will look into the areas of official sampling position and cutting area consisting of the Neck, Belly, and, Butt positions in the hide/skin.[28] The region of interest of the sorting person is mostly depending on the official sampling position on the hide or skin. Gogaev, O.K. and Demurova, A.R.,[29] had studied on thickness on the belly region and also mentioned about other regions such as neck, shoulder and thigh. Dagnew, N., et al.[30] studied differences between Butt, Neck and Belly Regions while making an assessment of histology and biochemical properties of sheep skin. Basil-Jones, M.M., et al.[31] measured edge-on the three positions namely Belly, official sampling position and, neck. In line with this, the current study has introduced a new method for defect detection on the five positions of the hide/skin namely Neck (N), Belly Left (BL), Belly Right (BR), Centre (C) and Butt (BT). The conventional sampling method is shown in Figure 4a and the proposed surface-based sampling is shown in Figure 4b.

Every pixel in each and every region was applied with binary threshold in identifying the boundaries of the particular shape which is otherwise called contours and stores the coordinates of row and column. Accordingly, the Class Label (C_i) for horizontal (Row_i) and vertical ($Column_j$) is calculated as shown in the Equation 2.

$$C_{ij} = (Row_i, Column_j \quad (2)$$

where C_i: Image Cropping in line with co-ordinates of i^{th} row and j^{th} column

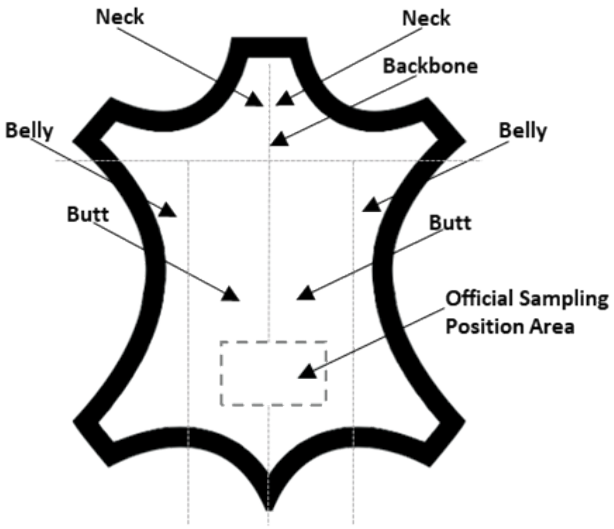

Figure 4a. Demarcated position of various regions within the hide for official sampling position

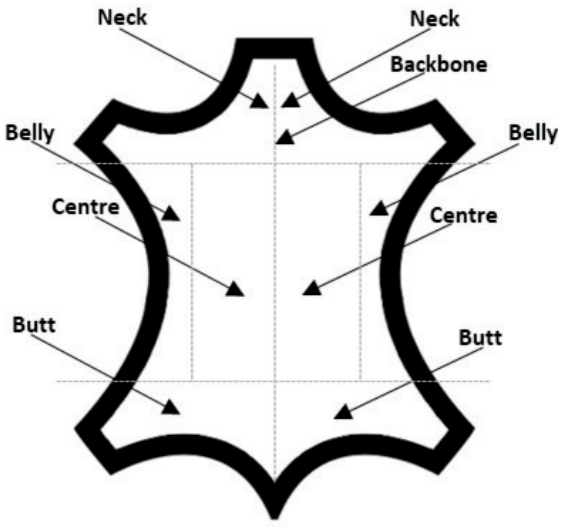

Figure 4b. Demarcated position of various regions within the hide for surface defect detection

Table I

Sample 6×6 Matrix representation of pixel points where i is row, j is column and n represent the size = 6

(1.1)	(1.2)	(1.3)	(1.4)	(1.5)	(1.6)
(2.1)	(2.2)	(2.3)	(2.4)	(2.5)	(2.6)
(3.1)	(3.2)	(3.3)	(3.4)	(3.5)	(3.6)
(4.1)	(4.2)	(4.3)	(4.4)	(4.5)	(4.6)
(5.1)	(5.2)	(5.3)	(5.4)	(5.5)	(5.6)
(6.1)	(6.2)	(6.3)	(6.4)	(6.5)	(6.6)

Table II

Representation of three region mapping of pixel point as Row Size (RS) = n/3

Region 1	Region 2	Region 3
Where i=1, j=1	Where i=RS, j=1	Where i=RS * 2, j=1
Row count start = i	Row count start = i	Row count start = i
Row cound end = RS	Row cound end = RS * 2	Row cound end = j
Column Count Start = i	Column Count Start = j	Column Count Start = j
Column Count end = j	Column Count end = n	Column Count end = n

The mapping of pixel points at each and every region is designed as shown in Table I and Table II for three regions. The image cropping is implemented for the Region 1, the i^{th} and j^{th} values are equal as it becomes the starting point, for the Region 2, i^{th} value becomes row size and j^{th} value as 1 as this is the mid-point and for the Region 3, the i^{th} value becomes row size multiplied by 2 and j^{th} value as 1 becomes last point.

Generation of Ranking Matrix:

In generation of ranking, the label values of Horizontal and vertical class values are mapped with the possible probabilities which is derived from the threshold value of the image. The cutting area is about 87.88% and as per the grading mentioned in the Table III, it fits in the grade 4.

Yeh et al.,[32] had suggested methods are contrast method through histogram, internal color level method, external color level method and fuzzy method is by establishing a demerit count between physical unusable area calculation and unusable region defect grouping based on the percentage share of unusable area. However, they have commented that there is no stable method and for classifying the wet blue hide have been done using the Table IV. As per the table, if the area is above 8750 pixels, the grade will be allotted as 4. Establishing a Demerit Count Reference Standard[33] for the Classification and Grading of Leather Hides.

Table III

Cutting area and corresponding Grading

Grade	Cutting Area
1	100 %
2	95%
3	90%
4	85%
5	80%
6	70%
R	<70%

Table IV

Intermittent Leather grading based on area of usefulness based on demerit count

Grade or Rank	Area of usefulness
1	<2500
2	2500 to <5000
3	5000 to < 8750
4	>= 8750

Algorithm I : Rank Calculation:

Step 1: Input ClassLabelHor, ClassLabelVer

Step 2: if ClassLabelHor and ClassLabelVer are same then ClassRank = either ClassLabelHor nor ClassLabelVer

Step 3: otherwise ClassRank will be maximum value of either ClassLabelHor nor ClassLabelVer

Label values of ClassLabelHor, and ClassLabelVer are derived based on the pixel intensity value associated with respect of the co-ordinates of horizontal (Row_i) and vertical ($Column_j$) as stated in Table V.

Grading Score on Image Position wise (GSIP) ranking the Crust leather image based on the Algorithm I. The ClassRank value is carried with the input value of Horizontal and Vertical as per the equation (3) and (4). GSIP is predominately considering the useful area present in the Center region. Accordingly, based on the possible probabilities of the N, BL, BR, C and BT, RankClass Label is created with the ranking such as 1, 2, 3, 4, 5, 6, 7 and 8.

$$\text{ClassLabelHor} = I < 2 \text{ where I is the intensity value} \quad (3)$$

$$\text{ClassLabelVer} = J < 5 \text{ where J is the intensity value} \quad (4)$$

Where I and J is represents P(N), P(BR), P(BR), P(C), P(BT), P(N), P(BR), P(BR), P(C), P(BT) which are Pixel intensity value of Neck, Belly Left, Belly Right, Centre and Butt respectively.

Table V

Ranking based on Pixel intensity value associated with the co-ordinates of horizontal (Row_i) and vertical ($Column_j$)

P(N) <=2 for horizontal <=5 for vertical	P(BL) <=2 for horizontal <=5 for vertical	P(C) <=2 for horizontal <=5 for vertical	P(BL) <= 2 for horizontal <=5 for vertical	P(BR) <= 2 for horizontal <=5 for vertical	ClassLabelHor / ClassLabelVer
Yes	Yes	Yes	Yes	Yes	1
Yes	Yes	Yes	Yes	No	2
Yes	Yes	Yes	No	Yes	2
Yes	Yes	Yes	No	No	3
Yes	No	Yes	Yes	Yes	2
Yes	No	Yes	Yes	No	3
Yes	No	Yes	No	Yes	3
Yes	Yes	Yes	No	No	4
No	Yes	Yes	Yes	Yes	2
No	Yes	Yes	Yes	No	3
No	Yes	Yes	No	Yes	3
No	Yes	Yes	No	No	4
No	No	Yes	Yes	Yes	3
No	No	Yes	Yes	No	4
No	No	Yes	No	Yes	4
No	No	Yes	No	No	5
Yes	Yes	No	Yes	Yes	6
Yes	Yes	No	Yes	No	7
Yes	Yes	No	No	Yes	7
Yes	Yes	No	No	No	8
Yes	No	No	No	No	8
Yes	No	No	Yes	Yes	6
No	Yes	No	Yes	Yes	7
No	No	No	No	No	8

Classification with Naive Bayes:

Shi, Y., et al.[34] had proposed a jamming identification scheme based on small data driven Naive Bayes classifier. For the classification using Naive Bayes classifier, the ranks are grouped into two cases, the first case as "within the acceptable Range" having the value less than or equal to 4 and the alternative case having the value more than 8 as "Not within the acceptable Range" corresponding to an image.

Results & Discussions

Initially the original crust image of Set I are applied with Canny Edge Detection and also filtered with Filters such as Laplacian, Median, Prewitt, Roberts, Sobel, Scharr. After which as stated in Table VI, the Contour of the images are identified on the five positions consisting of Neck, Belly Right, Belly Left, Butt and Center. Then each and every image is broken into five parts as per the anatomy of the animal to identify the Contour of five regions based on the horizontal and vertical coordinates.

Table VI

Coordinates for an image of 250 × 250

Region / Area	Row	Column	Height	Width
Neck	1	1	10	250
Belly Left side	1	11	200	50
Centre	50	11	200	150
Butt	1	211	40	250
Belly Right side	201	11	200	50

Table VII

Demarcated position of various regions within the hide for surface defect detection

Actual Image	Neck region	Belly Left side region	Centre region	Butt region	Belly Right side region
 (A)					
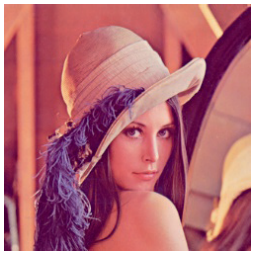 (B)			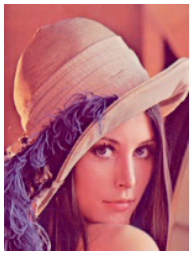		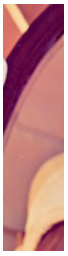
 (C)					
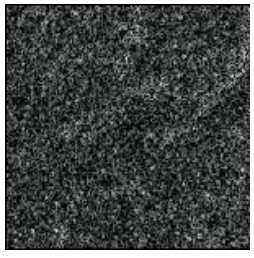 (D)					

Img	count_no_N	rowwisecount_N	count_no_BT	rowwisecount_BT	count_no_C	rowwisecount_C	count_no_BL	rowwisecount_BL	count_no_BR	rowwisecount_BR	ClassLabelHor	ClassLabelVer
1	2	37	1	5	1	37	1	5	1	5	1	7
2	1	5	1	5	1	5	1	5	1	5	1	1
3	1	5	1	5	1	5	1	5	1	5	1	1
4	1	5	1	5	1	5	1	5	1	5	1	1
5	5	36	3	5	1	260	1	140	2	82	3	8
6	1	40	1	117	1	57	1	85	1	18	1	8
7	8	57	1	224	1	249	1	110	1	92	2	8
8	3	5	1	73	1	64	2	153	1	45	2	8
9	1	5	1	5	1	25	1	42	2	25	1	8
10	1	5	1	27	1	5	1	62	1	5	1	3
11	1	5	1	5	1	20	1	5	1	5	1	6
12	2	9	1	18	1	12	1	10	1	5	1	8
13	1	5	1	18	1	5	1	5	1	5	1	2
14	1	5	1	5	1	5	1	5	1	5	1	1
15	1	5	3	277	4	122	4	156	1	33	8	8
16	1	5	1	14	1	5	1	10	1	5	1	3
17	1	5	1	5	1	5	1	5	1	5	1	1
18	2	17	2	90	3	20	1	13	1	63	6	8

Figure 5. output derived from the Algorithm I

The sample images of (A) Camera Man, (B) Leena, (C) Hide image and (D) Prewitt Filtered image are given in the table VII as per the demarcated position of various regions consisting of Neck region, Belly Left side region, Centre region, Butt region, and Belly Right side region.

The table VIII shows the Probabilities and various Position with Ranking Matrix of Dataset I and II generated from Algorithm I whereas initially the ranking is generated for Dataset I and it is observed from the Table VIII that the canny implemented Set I - Actual Images Applied with Canny confirms significantly working well over other dataset I filters with the Set I - Actual Images with Truth Values. Hence, in the dataset II, only the Canny edge detection is implemented and it also confirms significantly that out of 384 defect-based images to an extend of maximum. Once again it is confirming that the Canny edge detection-based filtering is significantly working well. A sample of the output is shown in Figure 5 Position with Ranking Matrix for the corresponding column and row of regions.

The Ranking of Dataset I and II are grouped into two categories namely within the acceptable range and not in the acceptable range which is derived from the ClassRank having less than 5. The GSIP is applied on the identified dataset is shown in Figure 6. According to the chosen dataset, the rank 8 covers maximum. The result shows that the defect classification with respect to Set I- Actual Images, Set I- Actual Images with Canny are better than of Set I – Laplacian Filter applied in Actual Image, Set I – Median Filter applied in Actual Image, Set I – Prewitt Filter applied in Actual Image, Set I – Roberts Filter applied in Actual Image, Set I – Sobel Filter applied in Actual

Table VIII

Ranking of Dataset I and II

Data Set I & II / Ranking	Rank 1	Rank 2	Rank 3	Rank 4	Rank 5	Rank 6	Rank 7	Rank 8
Set I - Actual Images with Truth Values	564	33	1	0	0	9	2	0
Set I - Actual Images Applied with Canny	0	0	92	504	4	1	0	8
Set I – Laplacian Filter Applied in Actual Image	54	6	3	1	1	4	0	540
Set I – Median Filter Applied in Actual Image	23	21	3	0	1	4	0	557
Set I – Prewitt Filter Applied in Actual Image	34	12	11	1	5	7	4	535
Set I – Roberts Filter Applied in Actual Image	51	10	7	2	1	6	4	528
Set I – Sobel Filter Applied in Actual Image	35	14	11	5	3	4	4	533
Set I – Scharr Filter Applied In Actual Image	39	10	7	2	2	5	1	543
Set -II - Defects Truth Values	37	16	7	1	1	5	3	314
Set -II - Defects Canny	0	1	0	0	0	0	0	383

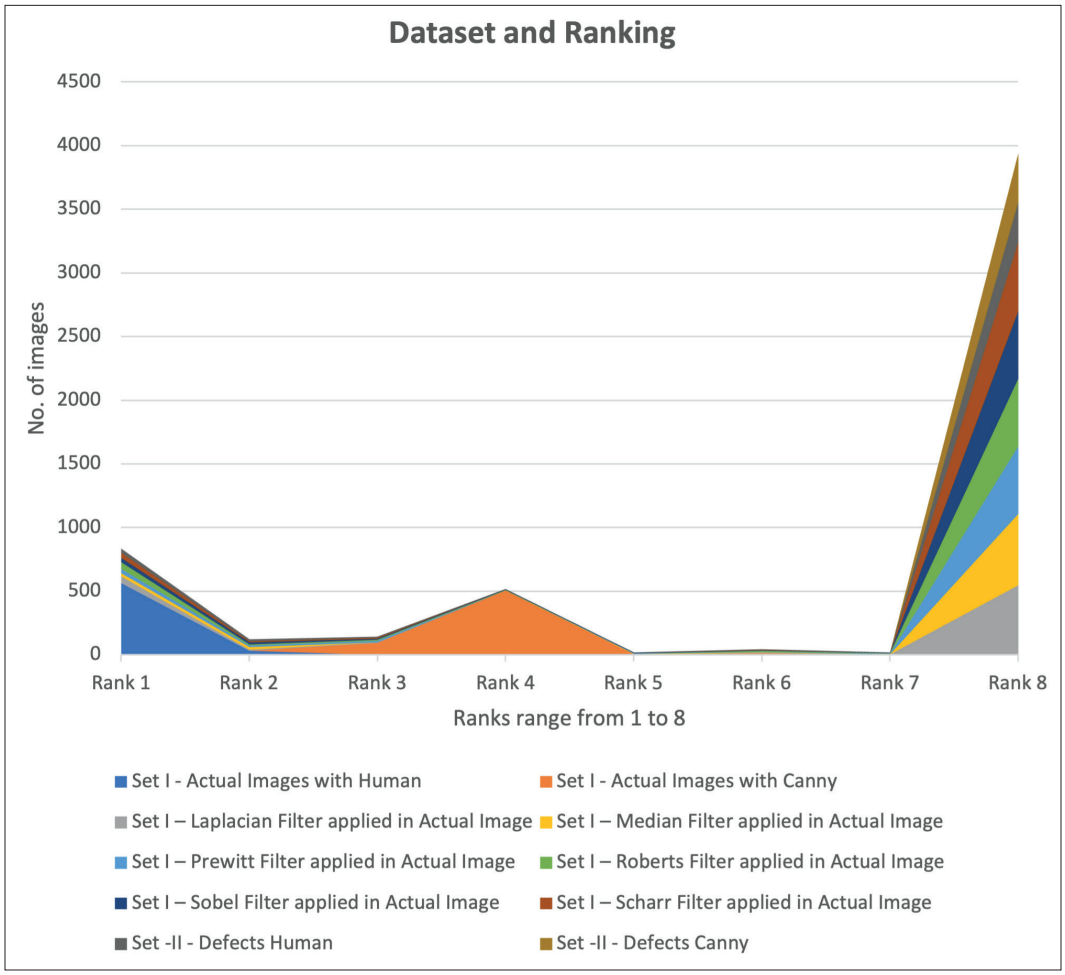

Figure 6. The GSIP chart of the dataset I and II

Table IX

Naïve Bayes Classifier Comparison of various image files

Dataset	Within acceptable range	Not within the acceptable range	Classification Accuracy
Set I - Actual Images with Human	598	11	0.99
Set I - Actual Images with Canny	596	13	**0.995**
Set I – Laplacian Filter applied in Actual Image	64	545	1
Set I – Median Filter applied in Actual Image	47	562	1
Set I – Prewitt Filter applied in Actual Image	58	551	0.985
Set I – Roberts Filter applied in Actual Image	70	539	0.99
Set I – Sobel Filter applied in Actual Image	65	544	0.99
Set I – Scharr Filter applied in Actual Image	58	551	0.99
Set -II - Defects Human	61	323	0.945
Set -II - Defects Canny	1	383	**0.995**

Image and Set I – Scharr Filter applied in Actual Image. In the case of Set II, classification of Set II – Actual Images and Set II – Actual Images with Defect implemented Canny.

Comparison of Naïve Bayes Classifier is shown in Table IX confirming the significant accuracy of Set I - Actual Images and Set II - Defects with implementation of canny edge detection over other image processing techniques at 99.50%. Moreover, among the filters applied in Set I, the sobel filter is also performing better than other filters at 91.17%. Hence, current study confirms that the proposed GSIP based ranking in detecting the surface based defect is significant as per the demarcated position of five regions within the hide for surface defect detection.

Conclusion

The proposed ranking matrix on the basis of demarcated position of five regions within the hide for surface defect detection namely Neck, Belly Left, Belly Right, Center, and Butt using Grading Score on Image Position wise (GSIP) is significantly performing as the accuracy of Set I - Actual Images and Set -II - Defects with implementation of canny edge detection over other image processing techniques at 99.50% for the dataset consisting of 5640 images using Naïve Bayes Classifier in this research article. Hence, current study confirms that the demarcated position of five regions and ranking would give an additional tool to inspectors while ranking the Crust leather.

Acknowledgments

Authors are thankful to University of Madras, Chennai and CSIR-Central Leather Research Institute (CSIR-CLRI), Chennai. The authors also sincerely acknowledging the support extended from Tanners Association and using of figures of CAMERA MAN and LEENA. The authors also acknowledge the CSIR-CLRI communication No. 1685.

References

1. International Trade Centre (ITC), Geneva, Switzerland, (https://www.intracen.org/itc/sectors/leather/)
2. Covington, A.D. and Wise, W.R.; Current trends in leather science. *Journal of Leather Science and Engineering*, **2**(1), pp.1-9, 2020.
3. Sathish, M., Aravindhan, R. and Rao, J.R.; Salt-free Chromium Tanning: Practical Approaches. *JALCA* **117**(1), pp.3-9, 2022.
4. Muthukrishnan, M., Jaimohan, S., Naresh, M.D., Ramesh, R. and Aravindhan, R.; A Non-destructive Evaluation of Fluffiness of Leather. *JALCA* **112**(08), pp.263-269, 2017.
5. Cooper, R.G.; Ostrich (Struthio camelus var. domesticus) skin and leather: A review focused on southern Africa. *World's Poultry Science Journal*, **57**(2), pp.157-178, 2001.
6. Gore, S.E., Laing, R.M., Lange, S., Scobie, D.R. and Young, S.R.; Changes to surface flaws on deer hides during processing to garment leather. *Journal of the Society of Leather Technologists and Chemists,* **86**(5), pp.183-7, 2002.
7. Gan, Y.S., Chee, SS., Huang, YC. et al.; Automated leather defect inspection using statistical approach on image intensity. *J Ambient Intell Human Comput* **12**, 9269–9285 (2021). https://doi.org/10.1007/s12652-020-02631-6
8. Liu, Y., Xie, Z., & Liu, H.; An adaptive and robust edge detection method based on edge proportion statistics. *IEEE Transactions on Image Processing*, **29**, 5206-5215, 2020.
9. Gandhi, M., Kamdar, J., & Shah, M.; Pre-processing of non-symmetrical images for edge detection. *Augmented Human Research*, **5**(1), 1-10, 2020.
10. Zhikang Xiao, Yang Zou, and Zhen Wang; An improved dynamic double threshold Canny edge detection algorithm, Proc. SPIE 11430, MIPPR 2019: Pattern Recognition and Computer Vision, 1143016 (14 February 2020); https://doi.org/10.1117/12.2539300
11. Li, B., He, F. and Zeng, X.; A novel privacy-preserving outsourcing computation scheme for Canny edge detection. The Visual Computer, pp.1-19, 2021.
12. Kumar, A.A., Lal, N. and Kumar, R.N.; A Comparative Study of Various Filtering Techniques. In 2021 5th International Conference on Trends in Electronics and Informatics (ICOEI), 26-31, IEEE. June 2021,
13. Aslam, M., Khan, T.M., Naqvi, S.S., Holmes, G. and Naffa, R., On the application of automated machine vision for leather defect inspection and grading: A survey. IEEE Access, **7**, 176065-176086, 2019.
14. Lai, K., Zhang, H. and Dai, D.; New approach to classification of surface defects in steel plate based on fuzzy neural networks. In Optical Information Processing Technology **4929**, 447-456. International Society for Optics and Photonics. September 2002.
15. Gong, R., Chu, M., Yang, Y. and Feng, Y.; A multi-class classifier based on support vector hyper-spheres for steel plate surface defects. *Chemometrics and Intelligent Laboratory Systems*, **188**, 70-78, 2019.
16. Hu, L., Zhou, M., Xiang, F. and Feng, Q.; Modeling and recognition of steel-plate surface defects based on a new backward boosting algorithm. The International *Journal of Advanced Manufacturing Technology*, **94**(9), 4317-4328, 2018.
17. Suvdaa, B., Ahn, J. and Ko, J.; Steel surface defects detection and classification using SIFT and voting strategy. *International Journal of Software Engineering and Its Applications*, **6**(2), 161-166, 2012.
18. Villar, P., Mora, M. and Gonzalez, P.; A new approach for wet blue leather defect segmentation. In Iberoamerican Congress on Pattern Recognition 591-598, Springer, Berlin, Heidelberg, November 2011.
19. Pistori, H., Paraguassu, W.A., Martins, P.S., Conti, M.P., Pereira, M.A. and Jacinto, M.A.; Defect detection in raw hide and wet blue leather. *In Proc. Int. Symp. CompIMAGE,* 355, May 2018.
20. Vasagam, S.N., Madhan, B., Chandrasekaran, B. and Rao, J.R.; 2013. Studies on Selective Defect Identification of Crust Leathers for Computer-aided Grading. *JALCA*, **108**(06), 210-220, 2013.

21. Liong, S.T., Zheng, D., Huang, Y.C. and Gan, Y.S.; Leather defect classification and segmentation using deep learning architecture. *International Journal of Computer Integrated Manufacturing*, 33(10-11), pp.1105-1117, 2020.
22. Jian, L., Wei, H. and Bin, H.; June. Research on inspection and classification of leather surface defects based on neural network and decision tree. In 2010 International Conference On Computer Design and Applications, 2, V2-381, IEEE, June 2010.
23. Bong, H.Q., Truong, Q.B., Nguyen, H.C. and Nguyen, M.T.; Vision-based inspection system for leather surface defect detection and classification. In 2018 5th NAFOSTED Conference on Information and Computer Science (NICS) 300-304, IEEE. November 2018.
24. Sornam, M. and Vasagam, S.N.; Surface Defect Identification and Grouping of Intermittent Leather Images using Linear Discriminant Model. *International Journal of Innovative Technology and Exploring Engineering*, **8**(12), 2253-2259, 2019.
25. Xie, X., Ge, S., Xie, M., Hu, F., Jiang, N., Cai, T. and Li, B.; Image matching algorithm of defects on navel orange surface based on compressed sensing. *Journal of Ambient Intelligence and Humanized Computing*, 1-9, 2018.
26. Aslam, Y., Santhi, N., Ramasamy, N. and Ramar, K.; Localization and segmentation of metal cracks using deep learning. *Journal of Ambient Intelligence and Humanized Computing,* 1-9, 2020.
27. Vasagam, S.N. and Sornam, M.; Intermittent Leather Defect Detection Based on Ensemble Algorithms Derived from Black Hat Transformation and Hough Transformation. *In ICT Analysis and Applications*, 35-45, Springer, Singapore, 2022.
28. 18 Covington, A.D.; Tanning chemistry: The Science of Leather. Royal Society of Chemistry, 2009.
29. 19 Gogaev, O.K. and Demurova, A.R.; Topographic features of sheep skin and coat structure. *Journal of Livestock Science* (ISSN online 2277-6214), **12**, 141-146, 2021.
30. Dagnew, N., Punitha, V., Sreeram, K.J., Rao, J.R. and Nair, B.U.; An Assessment of Differences between Butt and Belly Regions of Indian Sheep Skin. *JALCA*, **110**(06), pp.165-176, 2015.
31. Basil-Jones, M.M., Edmonds, R.L., Cooper, S.M., Kirby, N., Hawley, A. and Haverkamp, R.G.; Collagen fibril orientation and tear strength across ovine skins. *Journal of Agricultural and Food Chemistry*, **61**(50), 12327-12332, 2013.
32. S. Yeh C. and Perng D.; A Reference Standard of Defect Compensation for Leather Transactions. *The International Journal of Advanced Manufacturing Technology*, 1197 – 1204, 2005.
33. Yeh C. and Perng D. B.; Establishing A Demerit Count Reference Standard for the Classification and Grading of Leather Hides. *The International Journal of Advanced Manufacturing Technology*, **18**(10):731–738, 2001.
34. 22 Shi, Y., Lu, X., Niu, Y. and Li, Y., 2021. Efficient Jamming Identification in Wireless Communication: Using Small Sample Data Driven Naive Bayes Classifier. IEEE Wireless Communications Letters.